Electronic Supplementary Material (ESI) for Chemical Communications.
This journal is © The Royal Society of Chemistry 2015

Electronic Supporting Information

Improved oxidation of aromatic and aliphatic hydrocarbons using rate enhancing variants of P450Bm3 in combination with decoy molecules

Samuel D. Munday,[1] Osami Shoji,[2] Yoshihito Watanabe,[2] Luet-Lok Wong[3] and Stephen G. Bell[1,*]

Contents

Experimental

General reagents and organics were from Sigma-Aldrich, TCI, Acros or VWR. Buffer components, NADPH, and isopropyl-β-D-thiogalactopyranoside (IPTG) were from Astral Scientific and Biovectra, (Scimar, Australia). UV/Vis spectroscopy was performed on Varian Cary 5000 or Agilent Cary 60 spectrophotometers. Gas chromatography (GC) analyses were carried out on a Shimadzu GC-17A instrument coupled to a QP5050A MS detector using a DB-5 MS fused silica column (30 m x 0.25 mm, 0.25 μm) and helium as the carrier gas. Analytical liquid chromatography was performed using an Agilent 1260 Infinity pump equipped with an Agilent Eclipse Plus C18 column (250 mm x 4.6 mm, 5 μm), an autoinjector and UV detector (set at 220 nm). A gradient, 20 - 95%, of acetonitrile (with trifluoroacetic acid, 0.1%) in water (TFA, 0.1%) was used to elute the sample.

Activity assays

NADPH turnovers were run in 1200 μL of 50 mM oxygenated Tris, pH 7.4 at 30 ℃, containing 0.2 μM enzyme and 120 μg bovine liver catalase. Assays were held at 30 ℃ for 1 min prior to the addition of the decoy molecule (200 nM) was and the substrate (1 mM substrate from a 100 mM stock in DMSO). Finally NADPH was added, from a 20 mg mL^{-1} stock, to a final concentration of ~320 μM (equivalent to 2 AU). A period of 10 seconds was allowed to elapse after NADPH addition before the absorbance decay at 340 nm was measured. The reactions were allowed to run until all the NADPH was consumed. The NADPH turnover rate was derived using ε_{340} = 6.22 mM^{-1} cm^{-1}. All data are reported as the mean of at least three experiments.

Product analysis

After the NADPH consumption assays were completed, 990 μL of the reaction mixture was mixed with 10 μL of an internal standard solution (*trans*-4-phenyl-3-buten-2-one, 20 mM). The mixture was extracted with 400 μL of ethyl acetate and the organic extracts were used directly for GC-MS analysis. For the benzene-derived substrates, the oven temperature was

held at 60 ºC for 3 min and then increased at 10 ºC min^{-1} up to 140 ºC where it was held for 5 min then increased at 25 ºC min^{-1} to 220 ºC and maintained for 1 min. For cyclohexane, the oven temperature was started at 40 ºC for 6 min and then increased at 10 ºC min^{-1} to 120 ºC where it was maintained for 1 min then increased at 25 ºC min^{-1} to 220 ºC and held for 1 min. For HPLC analysis 134 μL of the reaction mixture was mixed 66 μL of acetonitrile before analysis.

The GC retention times for the substrates and products are given in Fig. S1 and S3. Products were identified by co-elution with authentic product standards or matching the GC-MS mass spectra to those expected for the standards (Fig. S1 and S3). Products were calibrated against standards using the assumption that isomeric products would give comparable responses e.g. 2,4-dimethylphenol and 2,5-dimethylphenol were presumed to give the same detector response.

Comparison of the structures of KT2 and decoy molecule bound BM3

The substrate-free crystal structure of the five-mutation KT2 variant of P450Bm3, which has generic activity-enhancing properties, has been determined to 1.9-Å resolution (PDB 3PSX).[1] There is a close resemblance to substrate-bound structures of the wild-type enzyme (WT). The disruption of two salt bridges that link the G- and I-helices in WT causes conformational changes that break several hydrogen bonds and reduce the angle of the kink in the I-helix where dioxygen activation is thought to take place. The side-chain of the key active site residue, Phe87 is rotated in one molecule of the asymmetric unit (but not the other), and the side-chains of Ile219, Phe158 and Phe261 cascade into the orientations found in fatty acid-bound forms of the enzyme. The iron is out of the porphyrin plane, towards the proximal cysteine. Unusually, the axial water ligand to the haem iron is not hydrogen-bonded to Ala264. As a result of these changes the rate of the first electron transfer from the reductase domain to the haem domain of substrate-free KT2 is almost as fast as in substrate-bound WT. However a significant alteration of the reduction potential of the haem domain is not observed. NADPH is turned over slowly by KT2 in the absence of substrate, so the catalytic cycle is gated by a step subsequent to the first electron transfer. This is different from the WT enzyme where the first electron transfer step is rate limiting in the absence of substrate. It is proposed that the generic rate accelerator properties of KT2 arise from the substrate-free form being in a catalytically ready conformation, such that substrate-induced changes to the structure play a less significant role in promoting the first electron transfer.[1]

No crystal structure with P450Bm3 has been obtained with PFC10 (K_d = 290 μM), PFC9 (K_d = 980 μM) or PFC8 (K_d = 1900 μM).[2,5] However the N-perfluoroacyl amino acid PFC9-L-Trp binds with higher affinity (K_d = 1.6 μM) and a structure of P450Bm3 bound to this substrate has been solved (PDB 3WSP).[2] Conformational changes are observed in this

structure providing evidence for a transition from the substrate free conformation of P450Bm3 to a more substrate bound-like conformation upon binding of the decoy molecule.

The overall structure of the decoy bound P450Bm3 has a quasi-open conformation in-between the open conformation and the closed substrate-bound conformations. Changes in the F and G helices and the F/G loop as well as in the I, H, and B′ helices and related loops are observed. This conformation provides space that allows access to an additional small substrate compared to the substrate bound form (N-palmitoylglycine, PDB 1JPZ).[3] Overall the short chain length of PFC9-L-Trp and therefore PFC8, PFC9 and PFC10 could accommodate substrates near the heme iron. One potentially important observation is that, water molecules, which are usually observed near the active site, even upon binding of long chain fatty acids (PDB 1JPZ and 1FAG),[4] are not observed. However, this may be related to the tryptophan moiety of PFC9-L-Trp rather than the PFC chain. Observed changes to important residues include Arg47, which is a polar residue close to the entrance of the substrate access channel. This residue moves toward the surface of the protein and away from the substrate. The orientation of Phe87, a key residue in the active site, is similar to that observed in the substrate-free structure (PDB 1BUZ) and one form of the KT2 structure but differs from the parallel orientation found in the N-palmitoyl glycine-bound structure (PDB 1JPZ).

Comparison of the changes across the structures of KT2 and PFC9-L-Trp reveals that in the decoy bound structure the Lys224-Asp251 and Asp217-Arg255 salt bridges which link the G helix to the I helix are intact. This is not the case in the KT2 and substrate bound structures. These alterations assist in reshaping the I helix of KT2 relative to the substrate free WT enzyme. The Ile219 and Phe261 residues of the PFC9-L-Trp bound structure are in similar positions to the WT enzyme but that of Phe158 occupies an orientation which resembles those of the KT2 mutant and the substrate bound forms of P450Bm3. In the active site the Phe87 residue moves only slightly away from the substrate free form in the decoy

bound structure the residues at Ala264 and Leu437 occupy a more substrate bound like orientation. This is particularly striking for Leu437 compared to its position in KT2. Overall both the KT2 and PFC9-L-Trp bound forms of P450Bm3 display certain features of the N-palmitoglycine bound structure.

In both KT2 and decoy bound P450Bm3 there are biochemical properties which are in agreement with these changes in the crystal structure. For example KT2 variant shows an enhanced rate of first electron transfer in the absence of substrate and faster NADPH oxidation rate in the presence of a substrate compared to the WT enzyme. The rate of NADPH consumption of P450Bm3 increases as PFC8, PFC9 and PFC10 are added (Table 1). In addition the longer the fluorinated fatty acid the tighter the binding.[2] This increase in affinity and activity as the chain length grows is in agreement with the preference of P450Bm3 for fatty acids which are C12-C18 in length. Optimal activity for P450Bm3 with saturated fatty acids is observed for pentadecanoic acid. The longer PFC fatty acids may induce more conformational changes which enhance the activity, yet still allow the second substrate to bind more efficiently in the active site of P450Bm3 (close to the heme).[2,5]

The decoy molecules are believed to improve the activity by a different yet similar mechanism to KT2. The addition of the decoy molecule to the WT, or the use of the KT2, improves the coupling efficiency over the WT enzyme (and the NADPH activity, Table 1 and Table 2).[5] Adding the decoy molecule to KT2 also improved the coupling. It is of note that there is no increase in the coupling for the KT2/decoy over the WT/decoy molecule combinations and there appears to be a ceiling on how high the coupling has been raised (Table 1 and Table 2). This may be due to ability of the decoy molecule to exclude excess solvent from the active site and limited by the orientation of the substrate in relation to the heme iron oxygen intermediates. Overall the KT2 and decoy molecule combination may only be able to enhance the coupling to a certain level which is governed by the binding of the

decoy molecule and the substrate in the active site rather than the conformational changes which appear to accelerate the activity of the rate determining step of the catalytic cycle. These changes do however allow for the enhanced activity when the two methods are combined (Table 1 and Table 2).

The data presented in Tables 1 and 2 shows that the decoy molecule method results in greater enhancement with the WT enzyme than KT2. This can be related to the conformational changes observed in the KT2 and decoy molecule bound enzymes. While the decoy molecule changes the conformation of WT to be in a more substrate bound like conformation the KT2 variant is already in a more substrate bound like conformation. Therefore the overall improvements for KT2 over the WT enzyme are less dramatic. The important observation is that the overall activity is still significantly greater than just using a decoy molecule with the WT enzyme.

In the PFC9-L-Trp bound structure there is space in the substrate binding pocket near the heme to accommodate another species and this is likely to also be true for the PFC8, PFC9 and PFC10 decoy molecules used here.[2] Critically our results show that the substrates must bind in the same orientation as the WT enzyme which results in the identical regioselectivity (Table S3).

Table S1 The area of the phenol and cyclohexanol product peaks and the internal standard (IS) for the turnovers of benzene and cyclohexane shown in Fig. 1.

Turnover	Phenol	IS	Ratio
WT + benzene	130709	33374207	0.0039
WT/PFC9 + benzene	2814013	26165368	0.11
KT2 + benzene	1073958	35451740	0.030
KT2/PFC9 + benzene	2531010	34350857	0.074

Turnover	Cyclohexanol	IS	Ratio
WT + cyclohexane	430974	36063091	0.012
WT/PFC9 + cyclohexane	17353849	53404483	0.32
KT2 + cyclohexane	12751020	52386615	0.24
KT2/PFC9 + cyclohexane	20774813	40760409	0.51

Table S2 *In vitro* turnover activity data for P450Bm3 variants and decoy molecule combinations with toluene, anisole, *p*-, *m*- and *o*-xylene. N = NADPH turnover rate; C = coupling efficiency (%); PFR = Product formation rate. Rates are given as nmol.(nmol P450)$^{-1}$.min^{-1}. All data are means of at least three experiments.

	WT	**WT+PFC8**	**WT+PFC9**	**WT+PFC10**	**KT2**	**KT2+PFC8**	**KT2+PFC9**	**KT2+PFC10**
toluene								
N	22 ± 0.9	159 ± 2	355 ± 3	622 ± 8	68 ± 2	282 ± 3	549 ± 7	822 ± 12
C	1.6 ± 0.5	28 ± 1	40 ± 1	25 ± 2	9.7 ± 3	31 ± 2	41 ± 1	33 ± 1
PFR	0.3 ± 0.1	44 ± 2	144 ± 3	158 ± 10	7 ± 2	90 ± 4	225 ± 8	271 ± 9
anisole								
N	122 ± 2	197 ± 2	262 ± 2	581 ± 3	189 ± 12	286 ± 8	399 ± 9	729 ± 16
C	1.4 ± 0.1	9.1 ± 1	18 ± 3	11 ± 0.5	7.5 ± 1	12 ± 0.8	19 ± 2	12 ± 0.1
PFR	2.0 ± 0.1	18 ± 2	48 ± 9	64 ± 3	14 ± 2	35 ± 3	76 ± 6	87 ± 2
***p*-xylene**								
N	63 ± 5	341 ± 2	687 ± 7	943 ± 7	267 ± 10	623 ± 10	1010 ± 33	1080 ± 8
C	19 ± 2	48 ± 2	56 ± 4	41 ± 4	34 ± 0.9	52 ± 1	54 ± 2	42 ± 2
PFR	12 ± 2	164 ± 7	386 ± 26	394 ± 35	90 ± 1	322 ± 13	549 ± 22	460 ± 26
***m*-xylene**								
N	33 ± 0.6	265 ± 4	546 ± 3	698 ± 8	178 ± 5	509 ± 2	830 ± 7	1050 ± 12
C	3.5 ± 0.4	48 ± 2	55 ± 1	40 ± 0.4	26 ± 2	48 ± 1	57 ± 2	43 ± 2
PFR	1.1 ± 0.1	129 ± 4	302 ± 5	278 ± 4	46 ± 4	244 ± 7	476 ± 15	455 ± 12
***o*-xylene**								
N	29 ± 1	160 ± 6	284 ± 5	468 ± 5	106 ± 2	380 ± 8	738 ± 18	1020 ± 16
C	1.9 ± 0.1	38 ± 1	53 ± 2	28 ± 2	30 ± 3	44 ± 3	45 ± 1	34 ± 1
PFR	0.6 ± 0.06	62 ± 4	149 ± 8	131 ± 6	32 ± 2	168 ± 14	334 ± 17	346 ± 10

Table S3 Product distributions arising from the turnovers of the P450Bm3 variant and decoy molecule combinations with toluene, anisole, *p*-, *m*- and *o*-xylene. The products from toluene were *o*-cresol, *p*-cresol and benzyl alcohol (BA); from anisole; 2-methoxyphenol (2-MP) and 4-methoxyphenol (4-MP); from *p*-xylene; 2,5-dimethylphenol (2,5-DMP), 2,4-dimethylphenol (2,4-DMP) and 4-methylbenzyl alcohol (4-MBA); from *m*-xylene; 3-methylbenzylalcohol (3-MBA), 2,4-dimethylphenol (2,4-DMP) and 2,6-dimethylphenol (2,6-DMP) and from *o*-xylene were 2-methylbenzylalcohol (2-MBA), 2,3-dimethylphenol (2,3-DMP), 3,4-dimethylphenol (3,4-DMP), 2,6-dimethylphenol (2,6-DMP), and 6,6-dimethylcyclohexa-2,4-dienone (6,6-DMCHD). Values are reported as the mean of at least three experiments. [a] Values reported for the WT enzyme are from the literature with the exception of those from *p*-xylene due to the reassignment of the product distribution. For the WT enzyme and *p*-xylene the levels of product formation were not sufficient to quantitate the levels of 4-methylbenzyl alcohol production accurately.

	WT[a]	**WT+PFC8**	**WT+PFC9**	**WT+PFC10**	**KT2**	**KT2+PFC8**	**KT2+PFC9**	**KT2+PFC10**
toluene[6]								
o-cresol	>95	95 ± 0.5	95 ± 0.3	94 ± 0.7	95 ± 0.7	95 ± 0.5	95 ± 0.7	95 ± 0.7
p-cresol	<1	2 ± 0.2	2.5 ± 0.04	3 ± 0.3	2 ± 0.3	2 ± 0.4	2 ± 0.2	2 ± 0.3
BA	3	3 ± 0.5	2.5 ± 0.3	3 ± 0.4	3 ± 0.5	3 ± 0.2	3 ± 0.2	3 ± 0.5
anisole[6]								
2-MP	>90	92 ± 1	92 ± 0.8	90 ± 0.8	92 ± 0.2	90 ± 0.1	89 ± 1	88 ± 1
4-MP	<10	8 ± 1	8 ± 0.8	10 ± 0.8	8 ± 0.2	10 ± 0.1	11 ± 1	12 ± 1
***p*-xylene**[a,7]								
2,5-DMP	85 ± 1	81 ± 1	81 ± 0.3	81 ± 2	77 ± 1	77 ± 0.3	78 ± 0.3	78 ± 1
2,4-DMP	15 ± 1	14 ± 1	14 ± 0.3	14 ± 2	17 ± 1	17 ± 0.4	16 ± 0.7	16 ± 2
4-MBA	n.d.	~5	~5	~5	6 ± 0.5	6 ± 0.2	6 ± 0.4	6 ± 0.5
***m*-xylene**[8]								
2,4-DMP	87	94 ± 0.05	94 ± 0.2	94 ± 0.5	91 ± 0.3	92 ± 0.3	92 ± 0.1	92 ± 0.2
2,6-DMP	11	6 ± 0.05	6 ± 0.2	6 ± 0.5	7 ± 0.3	6 ± 0.3	6 ± 0.1	6 ± 0.2
3-MBA	2	-	-	-	~2	~2	~2	~2
***o*-xylene**[8]								
2,3-DMP	27	22 ± 2	20 ± 0.6	20 ± 2	24 ± 2	25 ± 1	24 ± 0.6	24 ± 0.4
3,4-DMP	10	9 ± 1	9 ± 0.4	10 ± 1	11 ± 0.5	12 ± 0.3	12 ± 1	14 ± 0.3
2,6-DMP	8	6 ± 0.1	6 ± 0.2	6 ± 0.1	6 ± 0.06	6 ± 0.1	7 ± 0.6	8 ± 0.2
2-MBA	47	56 ± 3	59 ± 1	58 ± 3	53 ± 2	53 ± 2	53 ± 2	51 ± 0.4
6,6-DMCHD	8	6 ± 0.3	6 ± 0.5	6 ± 0.5	6 ± 0.5	4 ± 0.3	4 ± 0.1	3 ± 0.3

Scheme S1 Aromatic hydroxylation pathways in the oxidation of *p*-xylene. These shifts could also occur via the porphyrin mediated proton shuttle mechanism of aromatic oxidation proposed by Shaik and de Visser.[9]

Figure S1 Mass spectra of phenol and cyclohexanol products formed in the P450Bm3 turnovers.

benzene

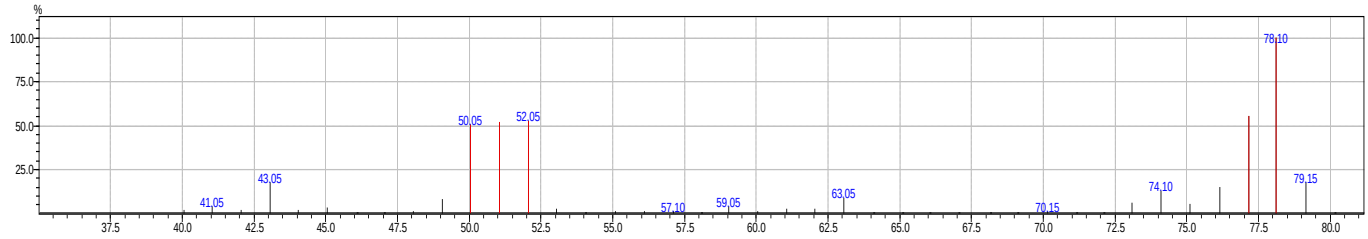

substrate, 1.56 min

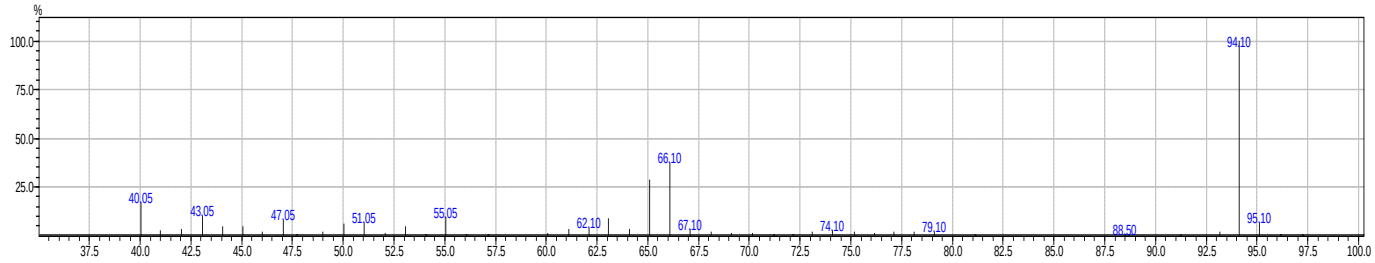

phenol: 5.4 min

cyclohexane

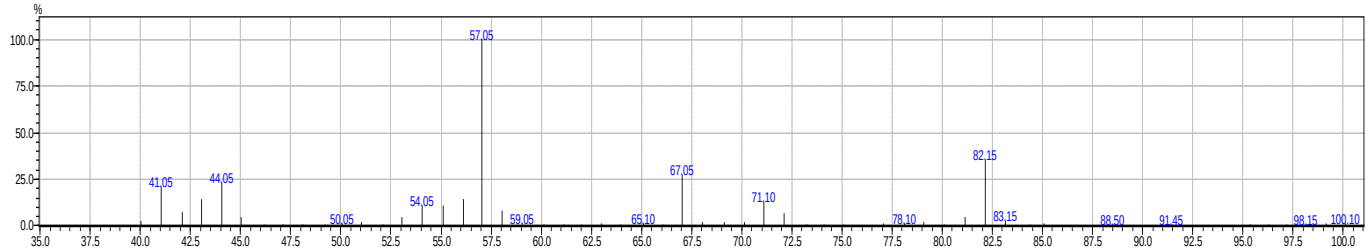

cyclohexanol, 7.5 min

a zoomed in version showing the peaks more clearly is shown below

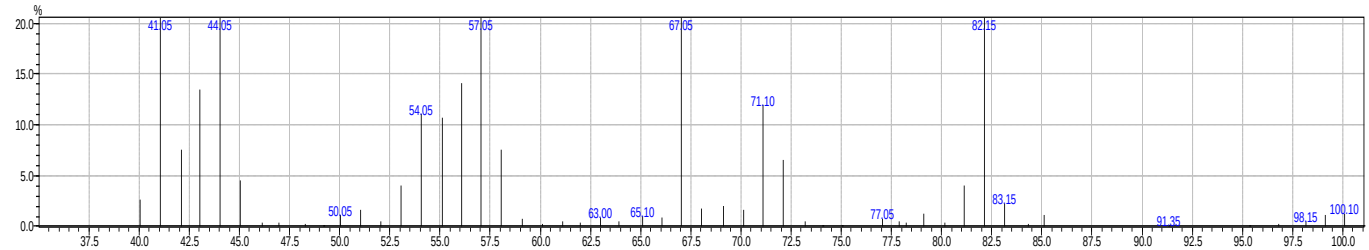

Figure S2 GC-MS analysis of the turnovers of (a) toluene, (b) anisole and (c) *m*-xylene using the WT and KT2 variants of P450Bm3 with and without the decoy molecules PFC8-PFC10.

(a)

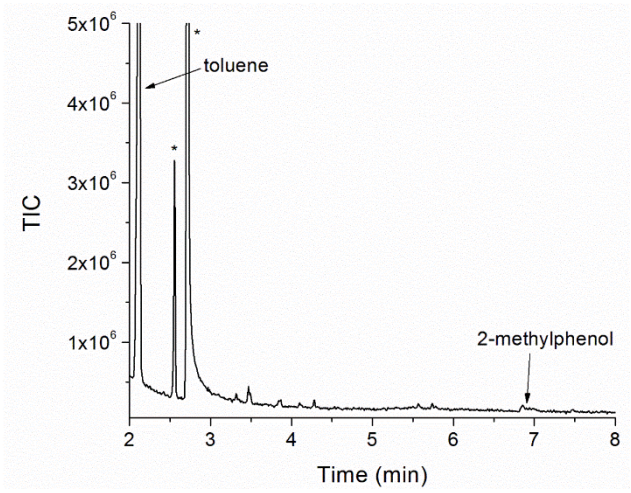

toluene-WT

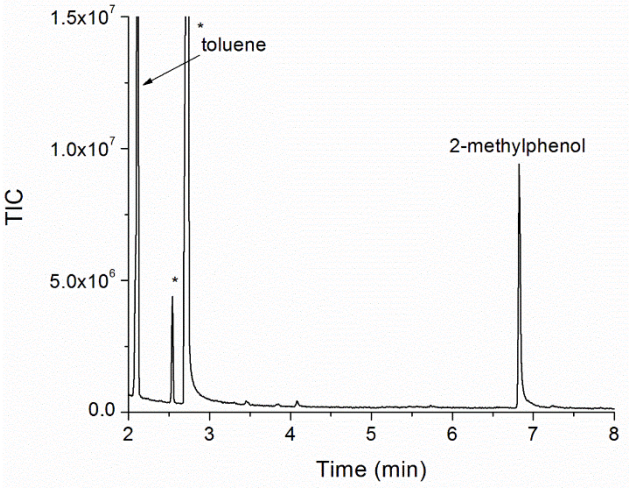

toluene-WT/PFC8

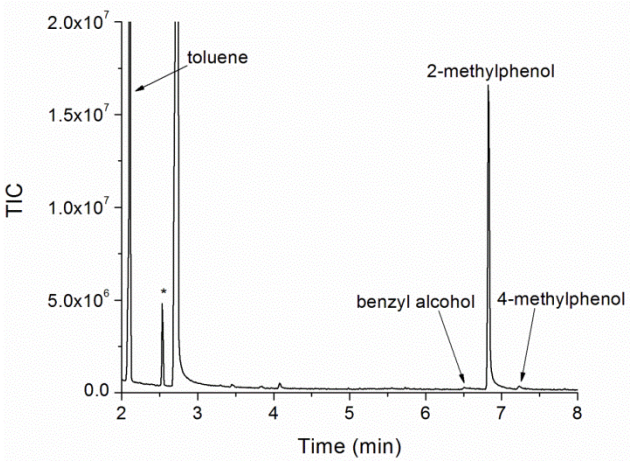

toluene-WT/PFC9

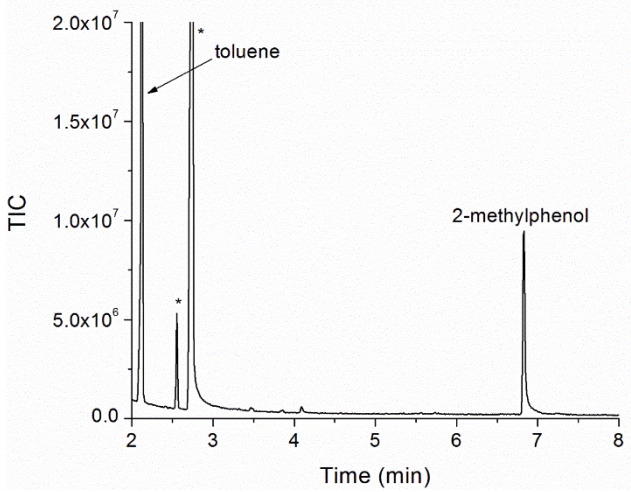

toluene-WT/PFC10

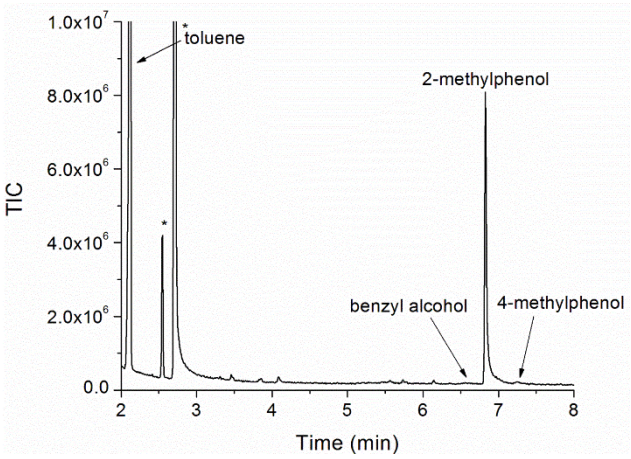

toluene-KT2

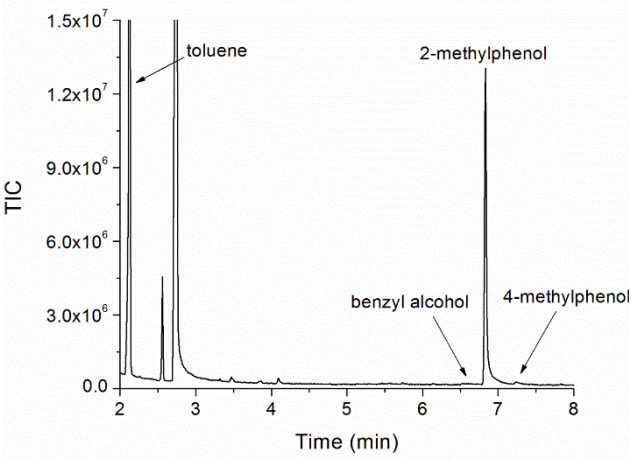

toluene-KT2/PFC8

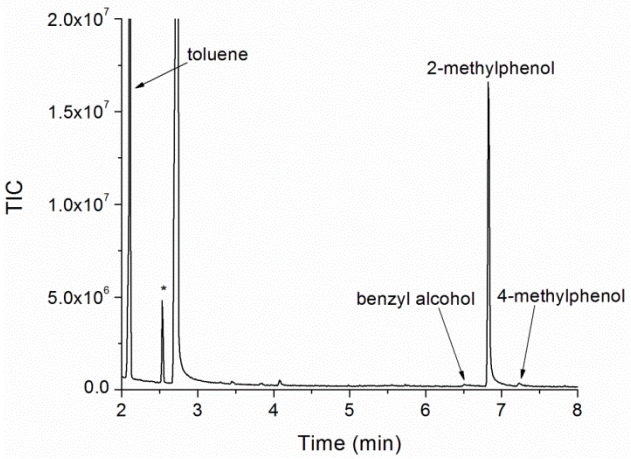

toluene-KT2/PFC9

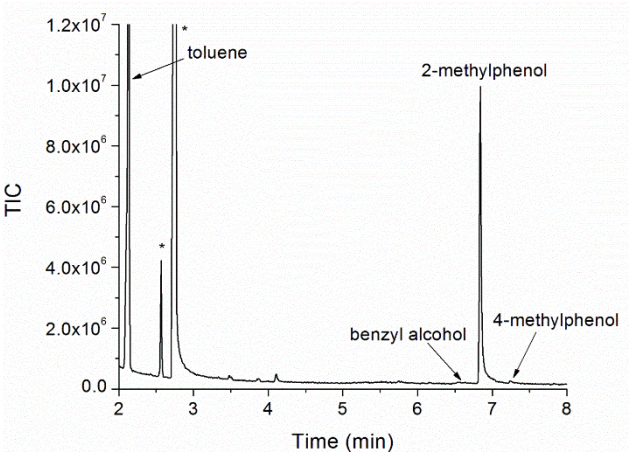

toluene-KT2/PFC10

(b)

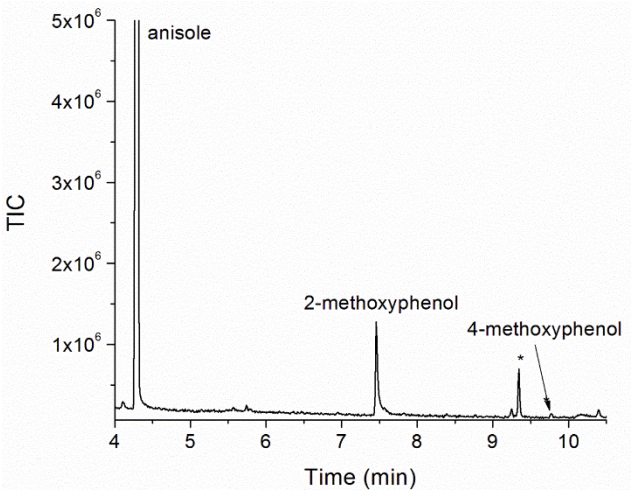

anisole-WT

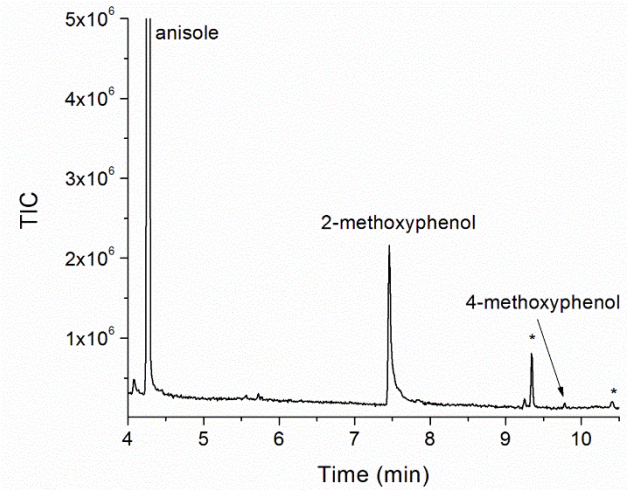

anisole-WT/PFC8

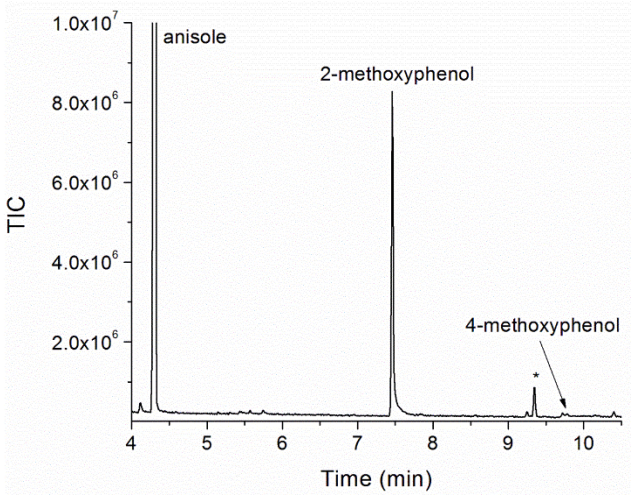

anisole-WT/PFC9

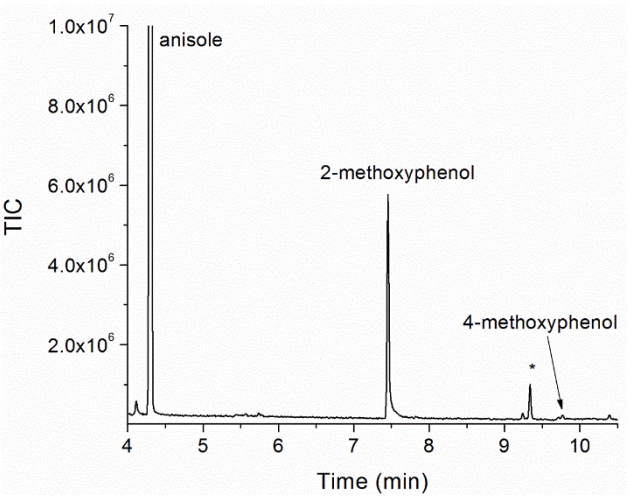

anisole-WT/PFC10

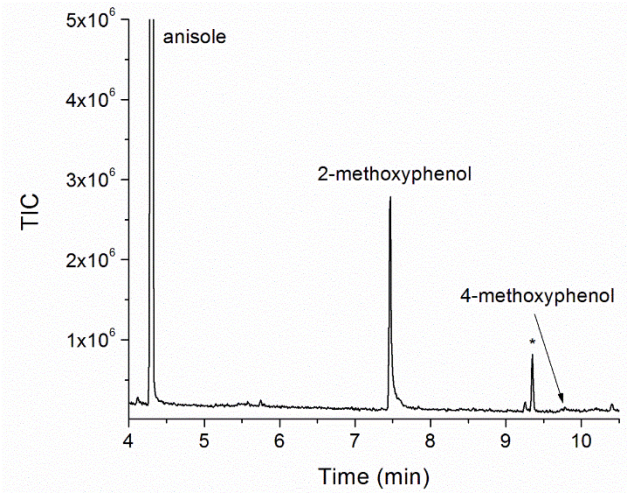

anisole-KT2

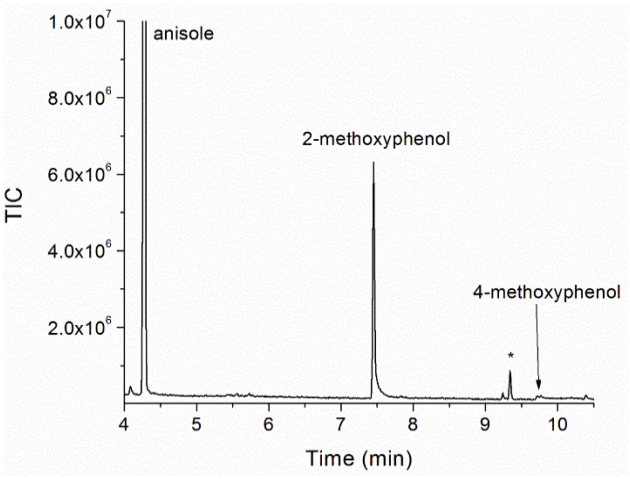

anisole-KT2/PFC8

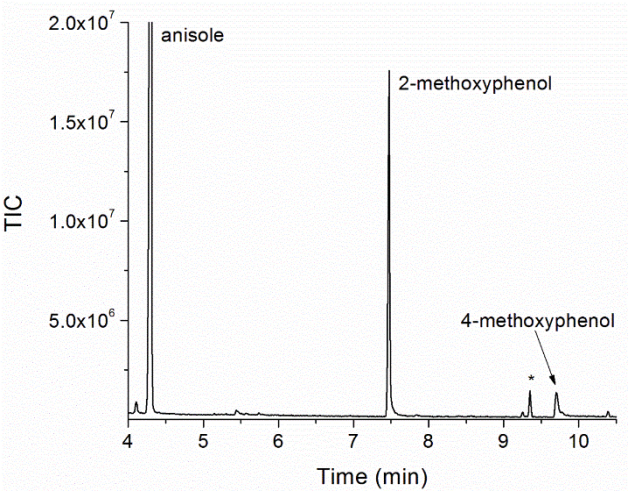

anisole-KT2/PFC9

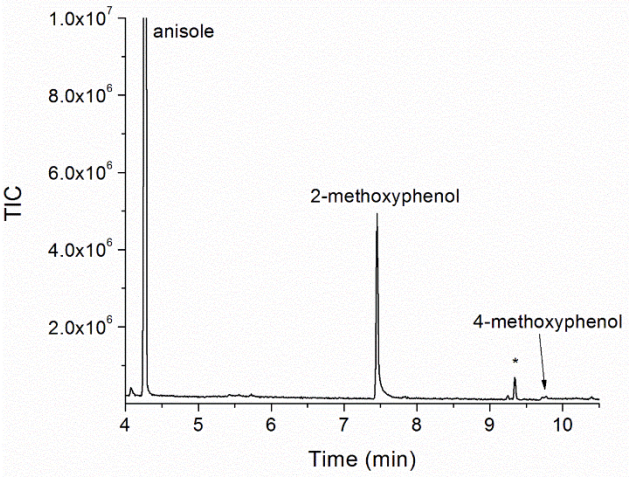

anisole-KT2/PFC10

(c)

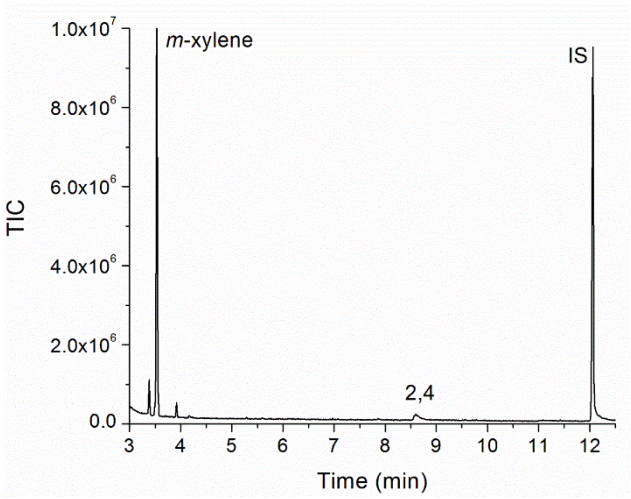

m-xylene-WT

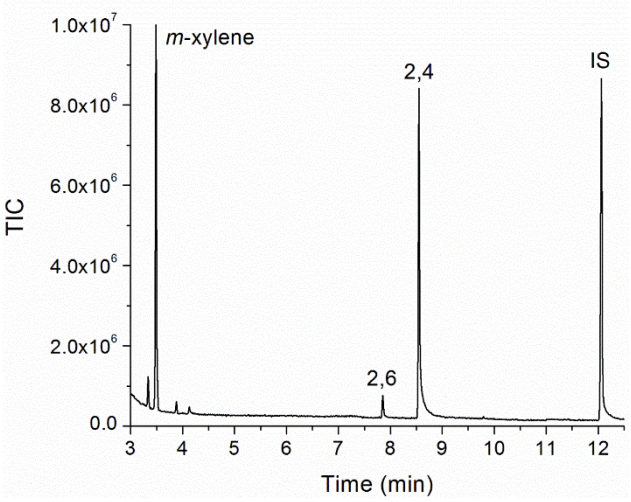

m-xylene-WT/PFC8

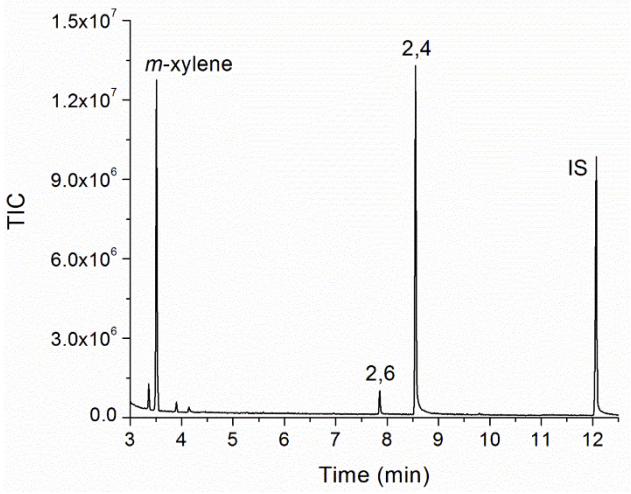

m-xylene-WT/PFC9

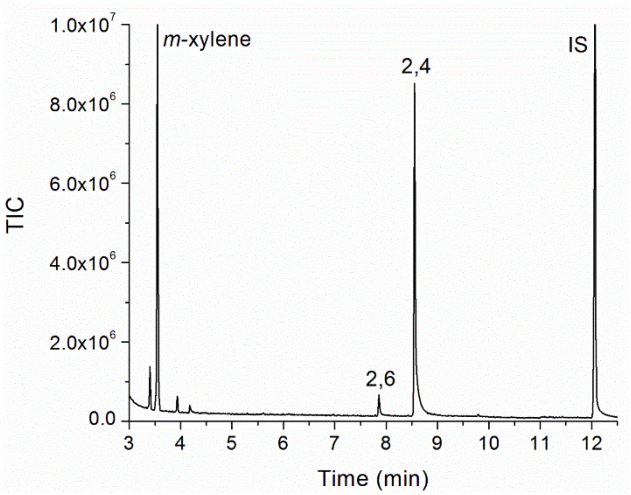

m-xylene-WT/PFC10

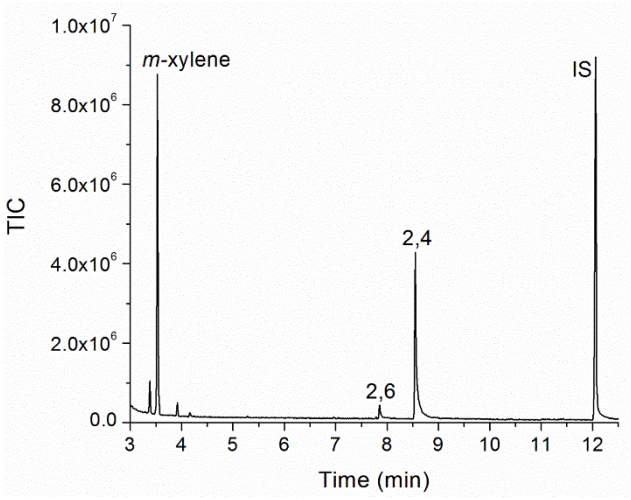

m-xylene-KT2

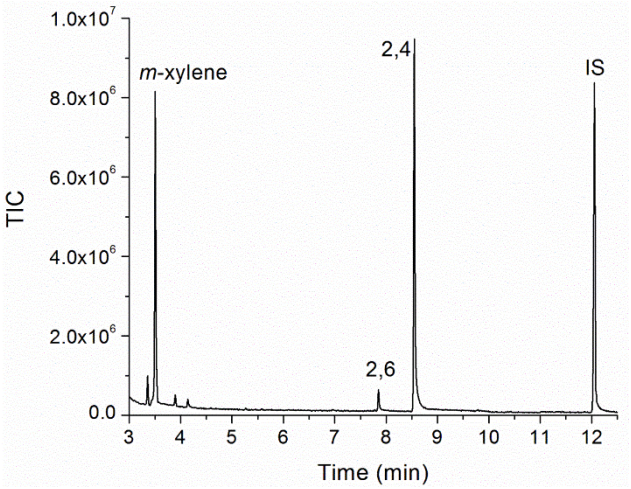

m-xylene-KT2/PFC8

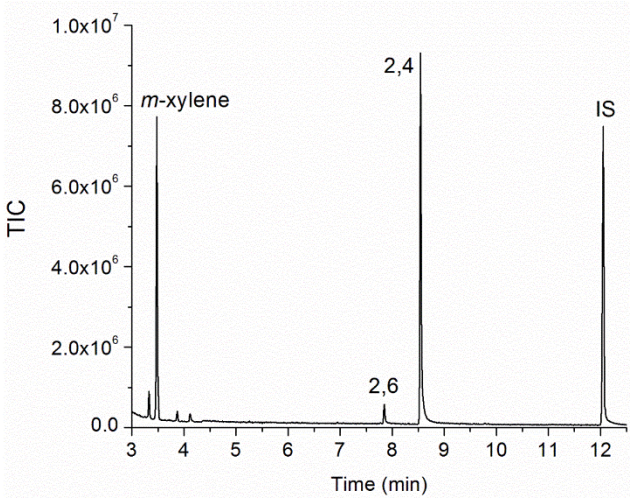

m-xylene-KT2/PFC9

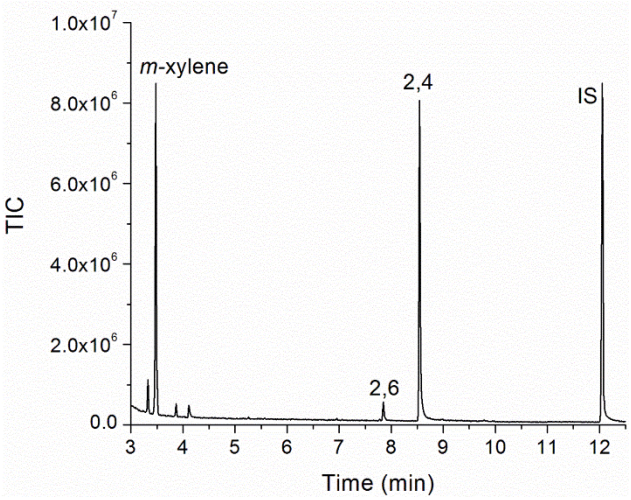

m-xylene--KT2/PFC10

Figure S3 Mass spectra of the substrates and products of the P450Bm3 turnovers of toluene, anisole, *o*-, *m*- and *p*-xylene.

toluene

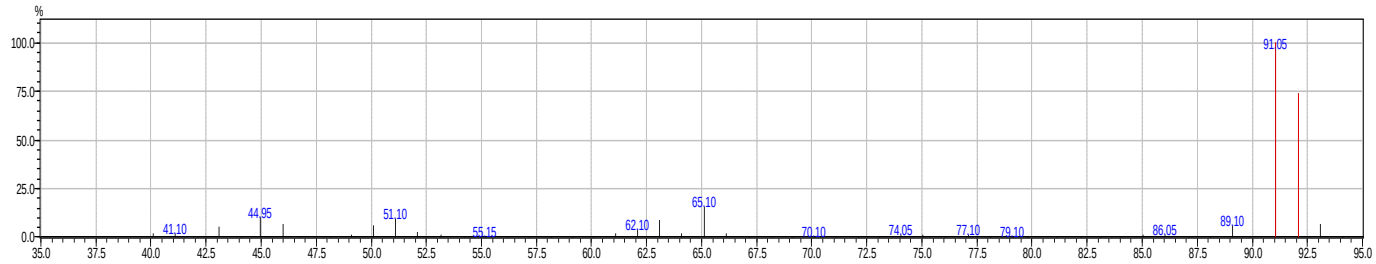

substrate, 2.1 min

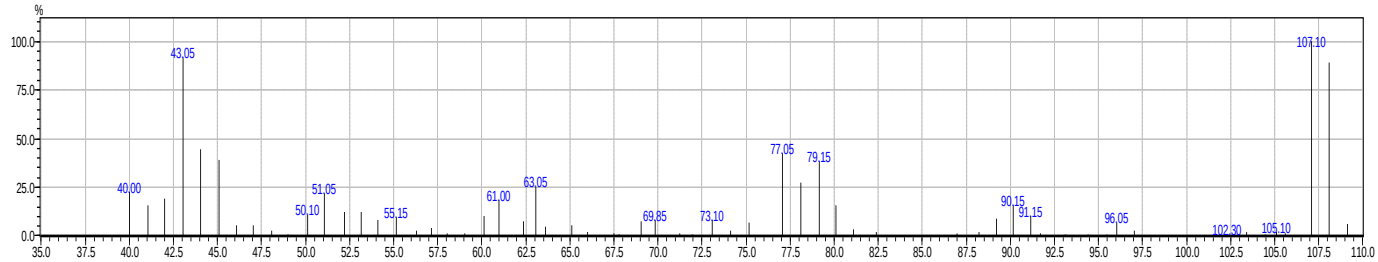

2-methylphenol (*o*-cresol), 7.1 min

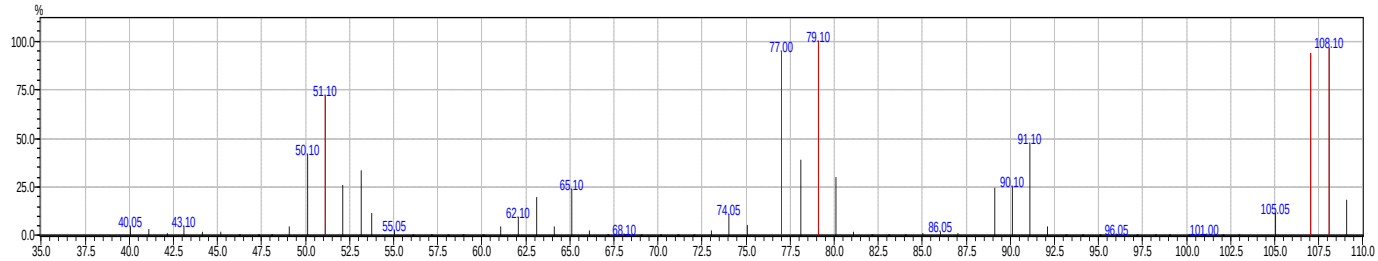

benzyl alcohol, 6.5 min

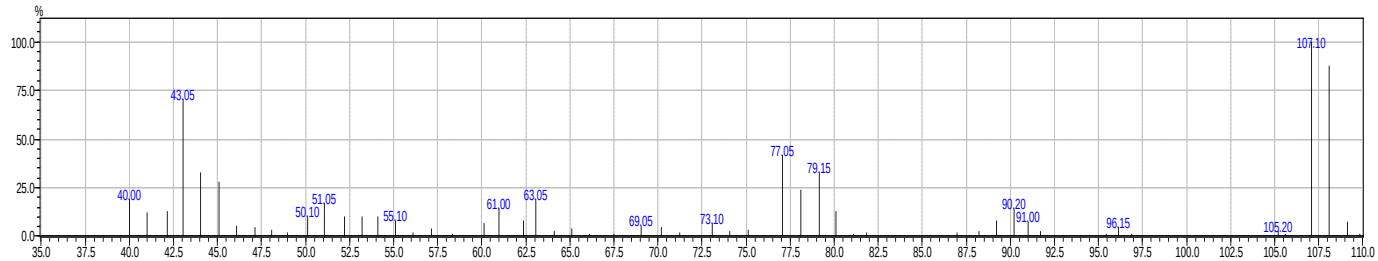

4-methylphenol (*p*-cresol): 7.2 min

anisole

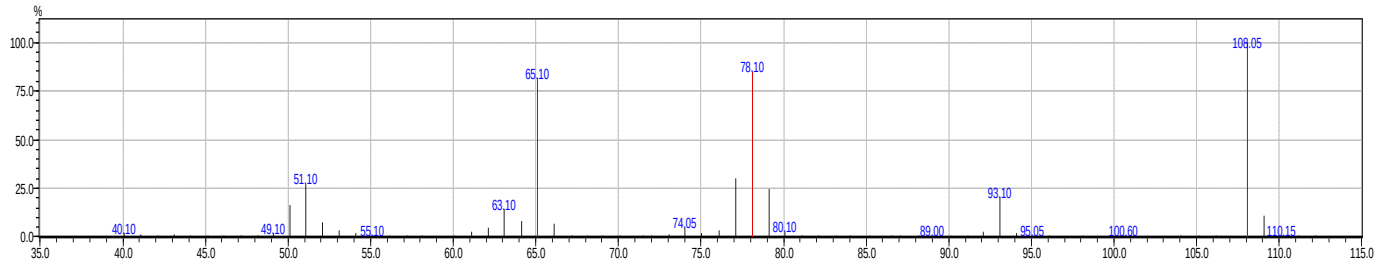

substrate, 4.3 min

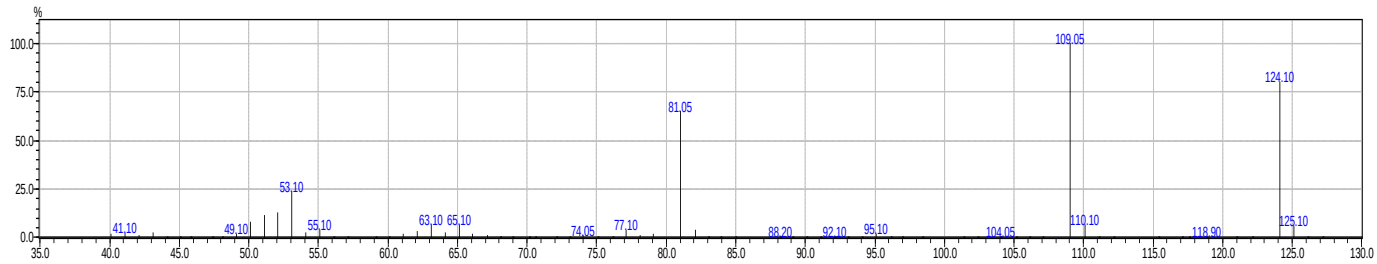

2-methoxyphenol (guaiacol): 7.45 min

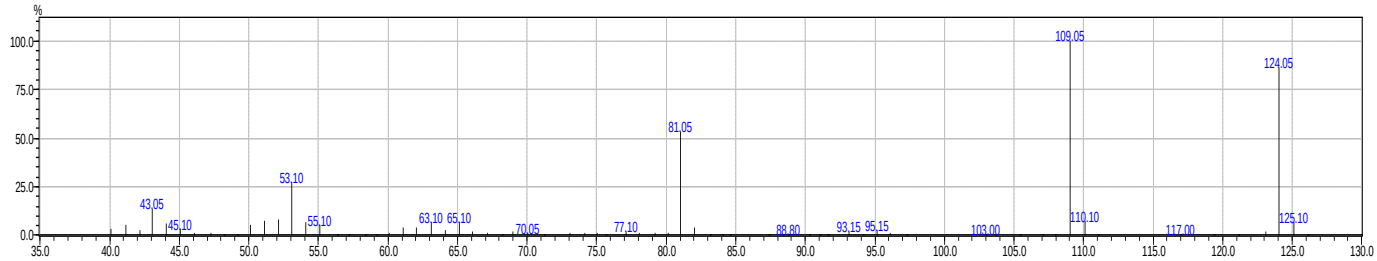

4-methoxyphenol, 9.7 min

***o*-xylene**

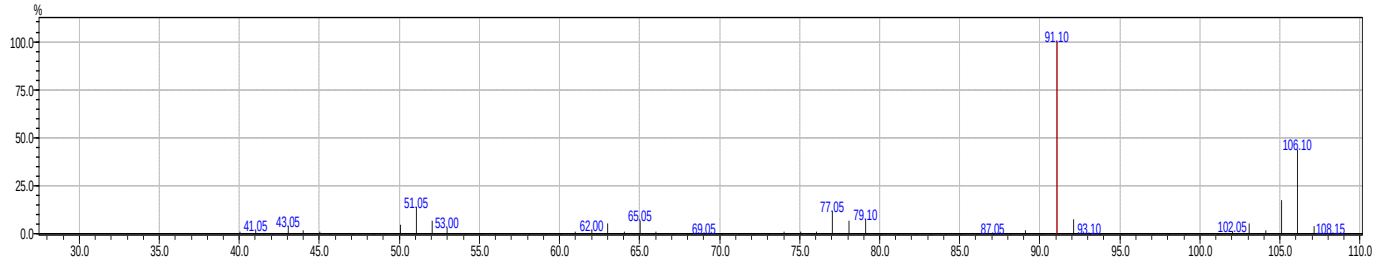

substrate, 3.9 min

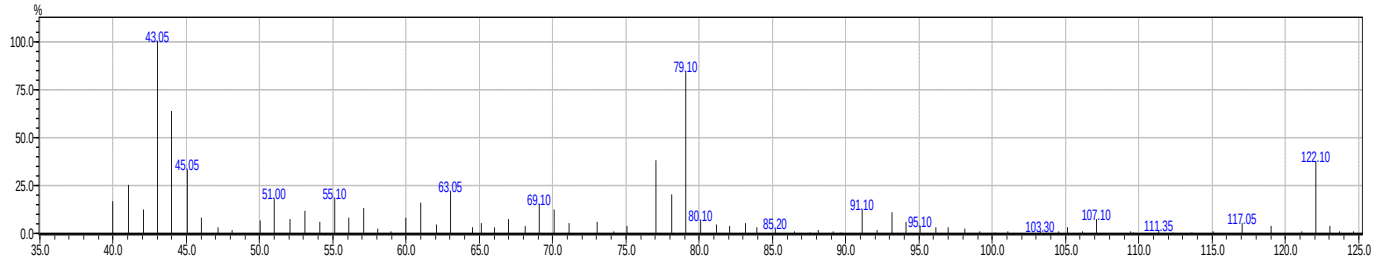

6,6-dimethylcyclohexa-2,4-dienone, 5.2 min

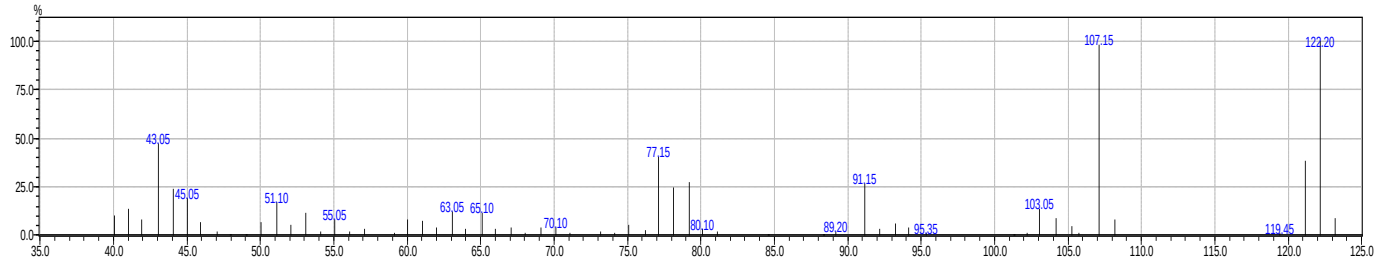

2,6 dimethylphenol, 7.8 min

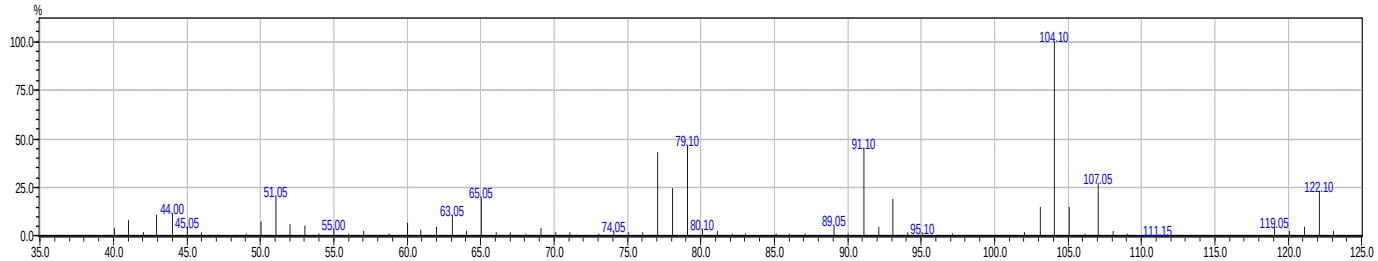

2-methylbenzyl alcohol, 8.5 min

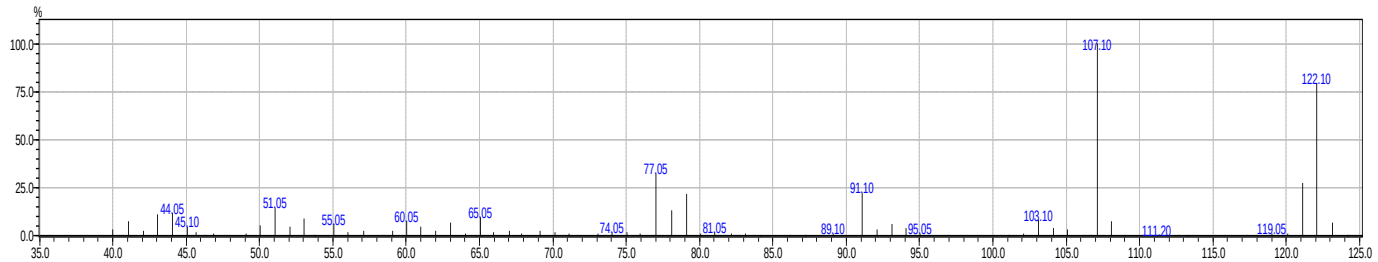

2,3-dimethylphenol, 9.0 min

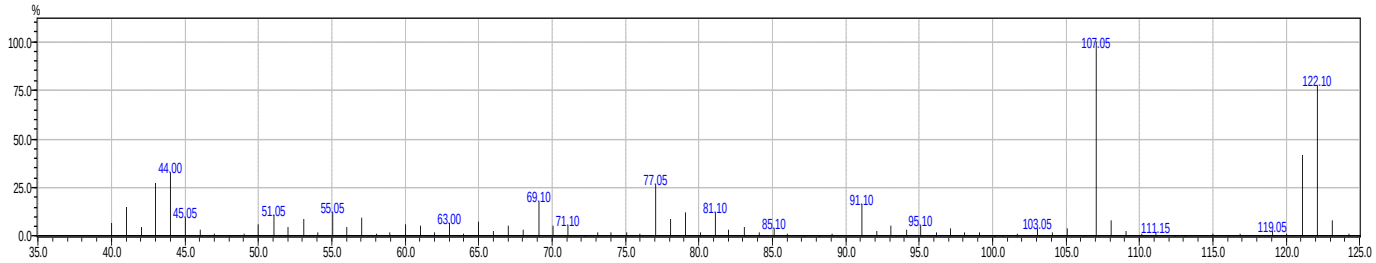

3,4-dimethylphenol 9.3 min

***m*-xylene**

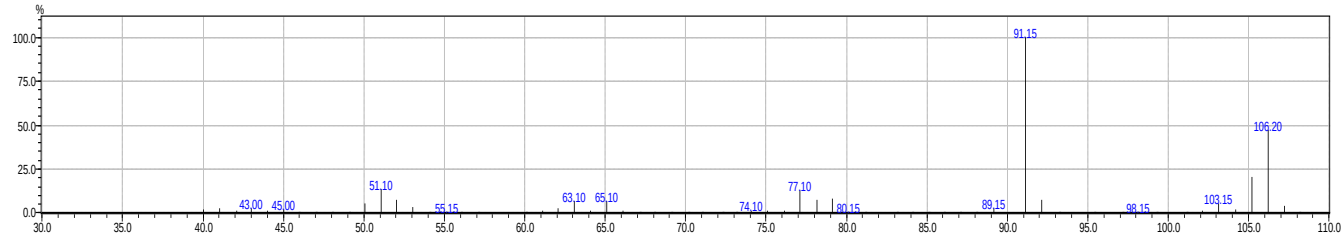

substrate: 3.5 min

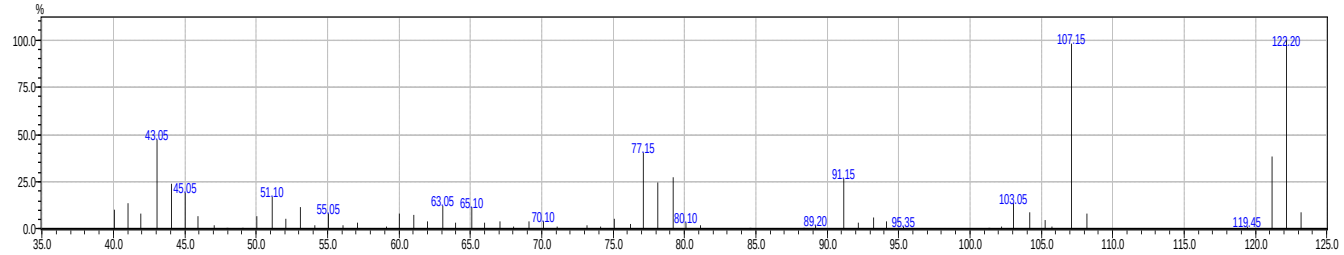

2,6-dimethylphenol, 7.8 min

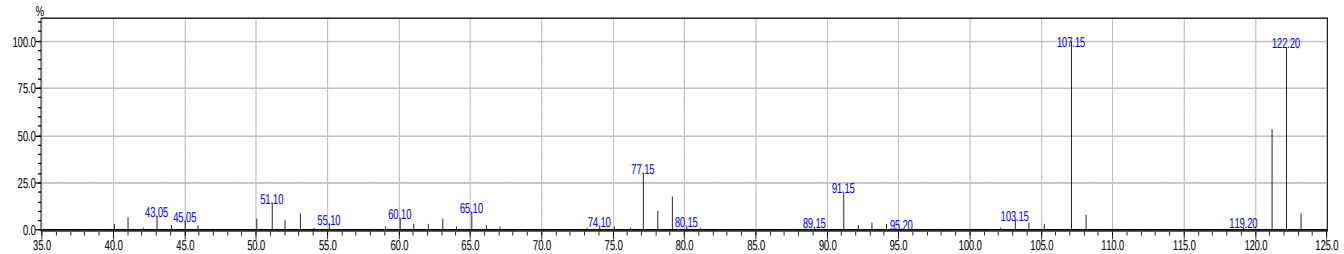

2,4-dimethylphenol 8.55 min

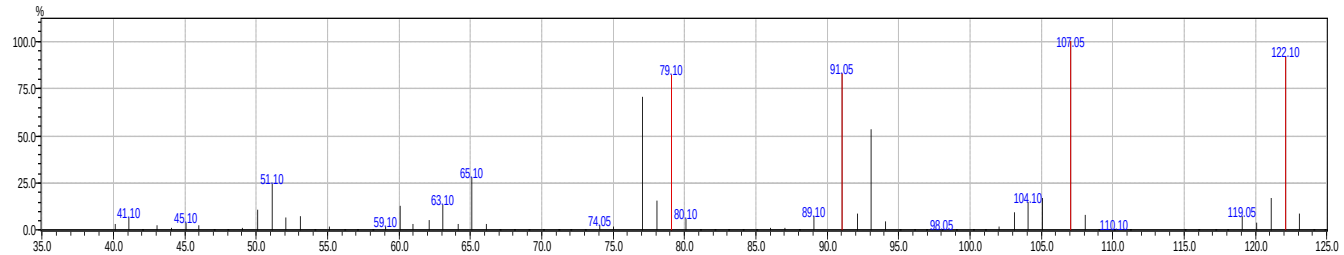

3-methylbenzylalcohol 8.4 min

***p*-xylene**

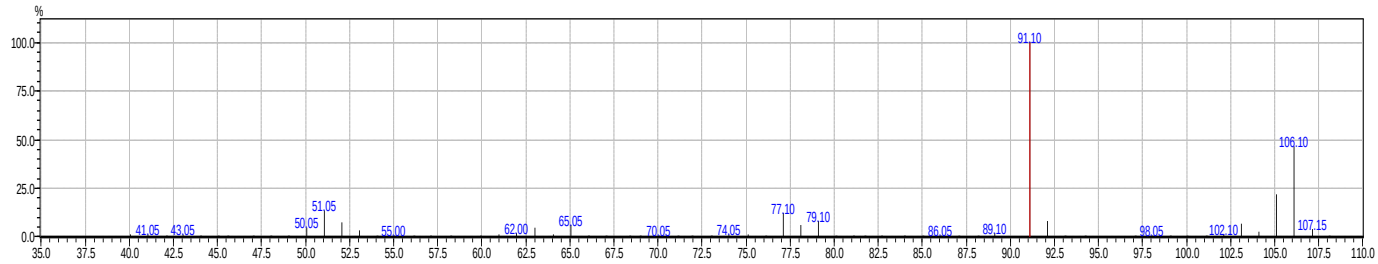

substrate, 3.5 min

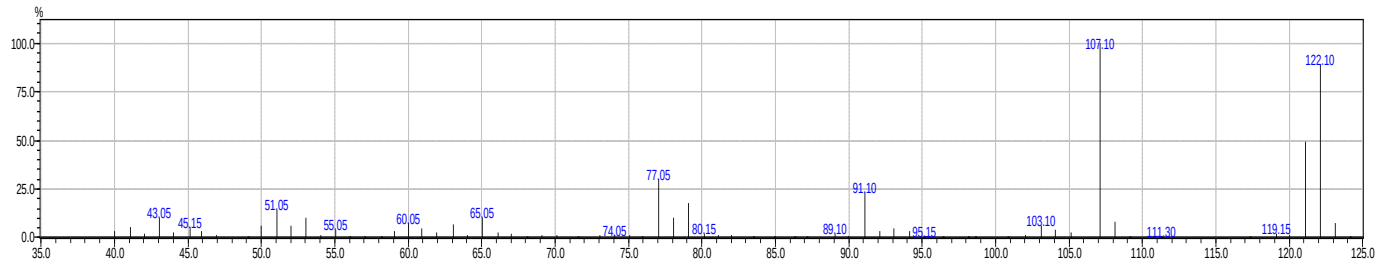

2,4-dimethylphenol, 8.55 min

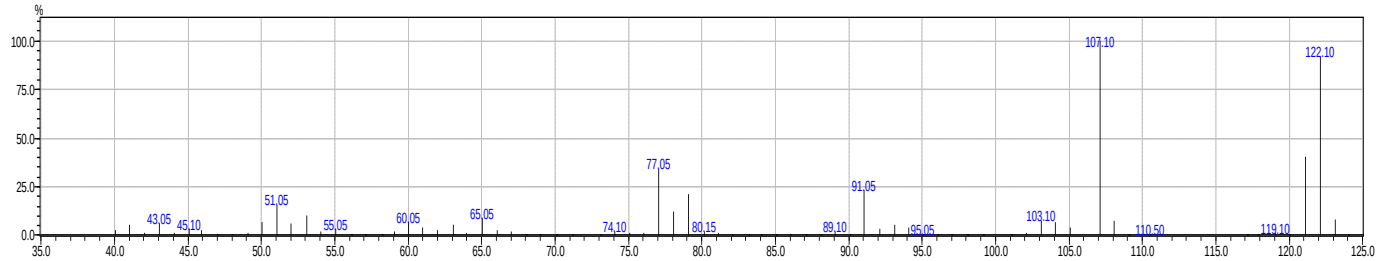

2,5-dimethylphenol: 8.6 min

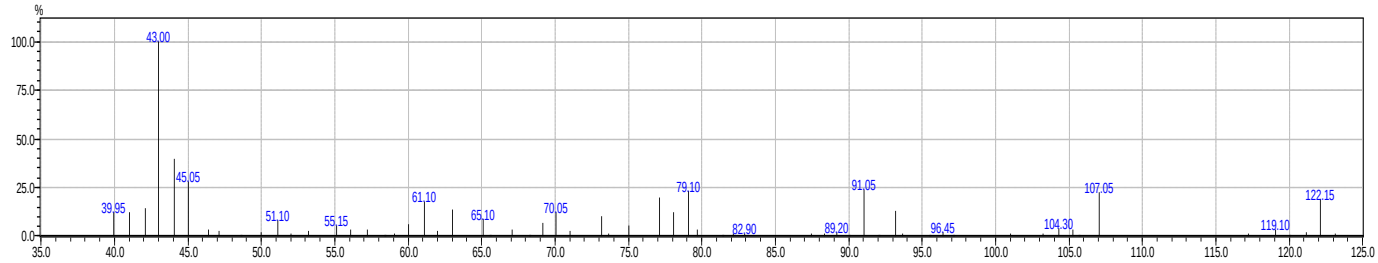

4-methylbenzylalcohol: 8.5 min

Figure S4 NADPH oxidation assays of (a) WT with *o*-xylene in the presence (red) and absence (black) of PFC10 and WT in the presence of PFC10 only (blue) (b) KT2 with *o*-xylene in the presence (red) and absence (black) of PFC10 and KT2 in the presence of PFC10 only (blue).

(a) (b)

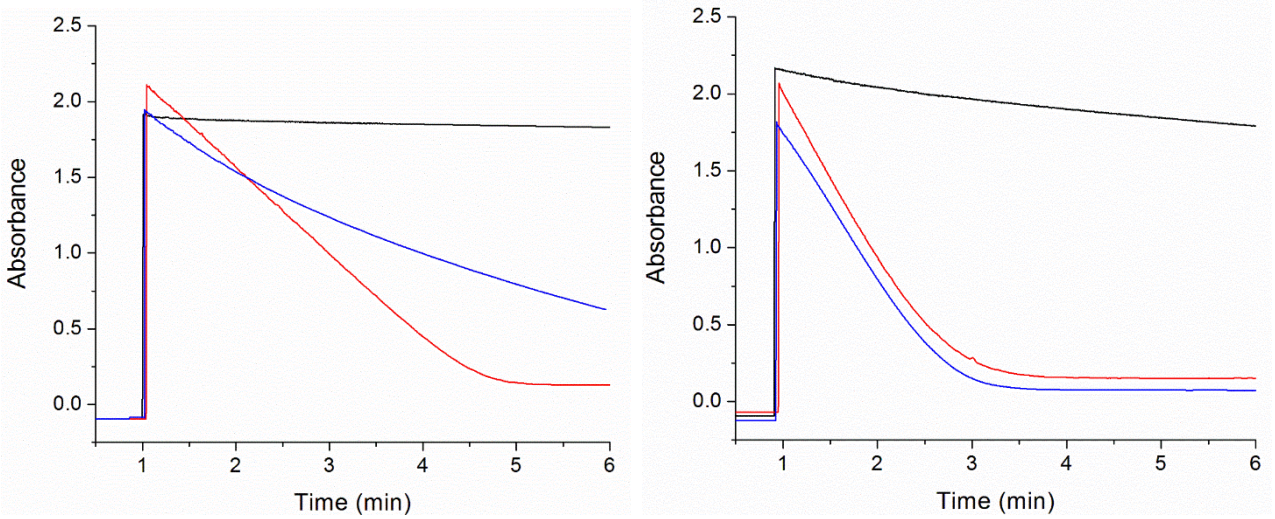

Figure S5 A zoomed in version of the product region of GC-MS analysis of the turnover of *p*-xylene with (a) KT2 and PFC8 and (b) the WT enzyme showing the different peaks due to the formation of 2,4- and 2,5-dimethylphenol.

HPLC analysis of (c) the turnover of WT/PFC10 with *p*-xylene. The turnover is in black, controls of 4-methylbenzyl alcohol (4MBA, Blue), 2,4-dimethylphenol (2,4-DMP, red) and 2,5-dimethylphenol (2,5-DMP, green); (d) the turnover of KT2/PFC9 with *m*-xylene. HPLC of *m*-xylene with KT2 + PFC9. The turnover is in black with controls of 3-methylbenzyl alcohol (3MBA, blue), 2,4-dimethylphenol (2,4-DMP, red) and 2,6-dimethylphenol (2,6-DMP, green). All monitored at 220 nm.

(a)

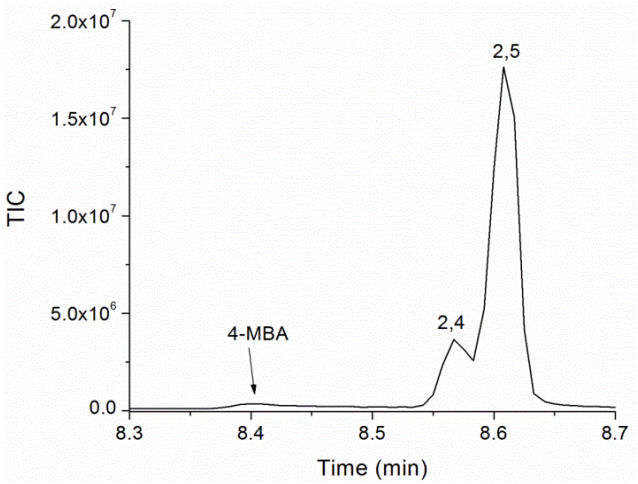

(b)

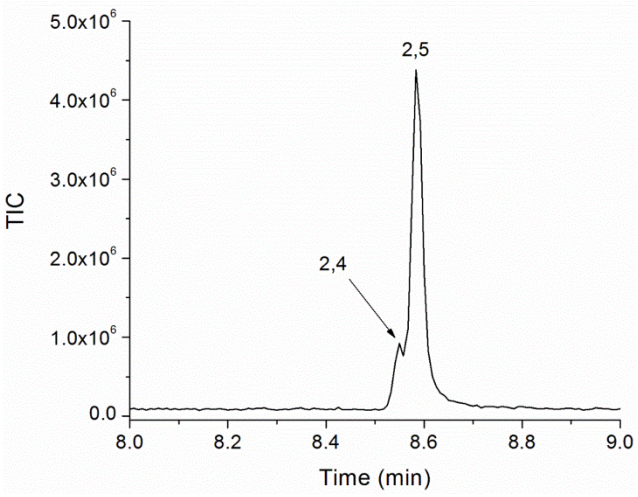

(c)

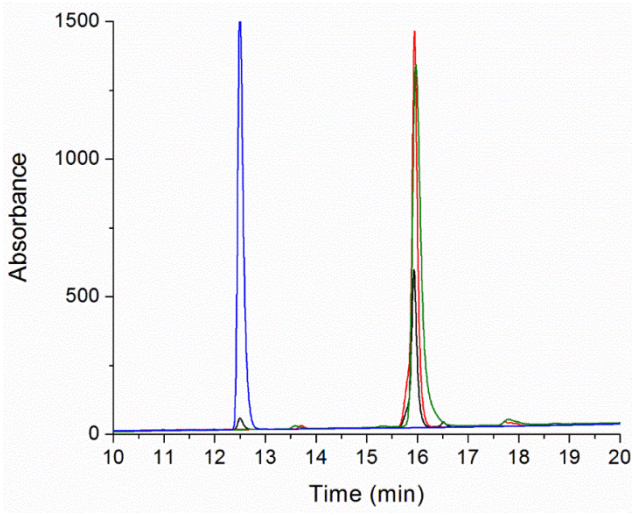

(d)

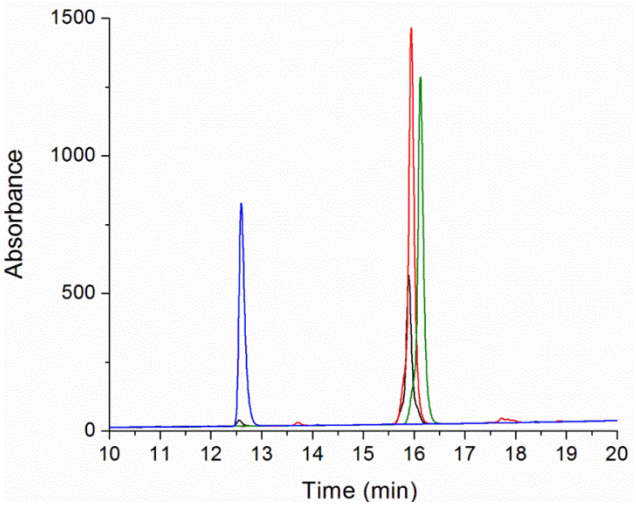

References

1. C. J. Whitehouse, W. Yang, J. A. Yorke, H. G. Tufton, L. C. Ogilvie, S. G. Bell, W. Zhou, M. Bartlam, Z. Rao and L. L. Wong, *Dalton Trans.*, 2011, **40**, 10383-10396.
2. Z. Cong, O. Shoji, C. Kasai, N. Kawakami, H. Sugimoto, Y. Shiro and Y. Watanabe, *Acs Catalysis*, 2015, **5**, 150-156.
3. D. C. Haines, D. R. Tomchick, M. Machius and J. A. Peterson, *Biochemistry*, 2001, **40**, 13456-13465.
4. H. Li and T. L. Poulos, *Nat. Struct. Biol.*, 1997, **4**, 140-146.
5. O. Shoji and Y. Watanabe, *Israel Journal of Chemistry*, 2015, **55**, 32-39.
6. A. Dennig, N. Lulsdorf, H. Liu and U. Schwaneberg, *Angew. Chem. Int. Ed. Engl.*, 2013, **52**, 8459-8462.
7. A. Dennig, J. Marienhagen, A. J. Ruff, L. Guddat and U. Schwaneberg, *ChemCatChem*, 2012, **4**, 771-773.
8. C. J. Whitehouse, N. H. Rees, S. G. Bell and L. L. Wong, *Chem. Eur. J.*, 2011, **17**, 6862-6868.
9. S. P. de Visser and S. Shaik, *J. Am. Chem. Soc.*, 2003, **125**, 7413-7424.